Mariusz MAŚLAK[1]
Michał PAZDANOWSKI[2]

INFLUENCE OF THE END-PLATE THICKNESS ON THE STEEL BEAM-TO-COLUMN JOINT STIFFNESS WHEN SUBJECT TO BENDING

Based on the numerical simulation performed within the Abaqus computational environment for a typical end-plate beam-to-column joint the influence of the end-plate thickness on the effective joint rigidity has been verified. The initial joint rigidity at first determined for 20 mm thick end-plate has been compared with rigidity of the joint constructed with substantially more flexible end-plates 10, 8 and 6 mm thick. In all the considered cases the column was equipped with horizontal ribs stiffening the web at the height of beam top and bottom flange. No diagonal ribs were applied. In addition the column flange at the zone directly adjacent to the beam end-plate in all the analyzed cases has been set to 30 mm. This way it did not affect the computationally determined rigidity of considered joints. Juxtaposition of M-φ curves characterizing the considered joints and depicting the relationship between the applied bending moment and relative change of the initial angle between undeformed axes of beam and column in the analyzed frame indicates qualitatively different modes of destruction of the considered joints, and thus different computational models determining their bearing capacity. In the first case obtained parameters seem to indicate that the joint is nominally rigid but in all the remaining cases the bearing capacity seems to be exhausted by the increasing deformation of the more and more flexible end-plate.

Keywords: beam-to-column steel end-plate joint, end-plate thickness, joint flexibility, initial stiffness, numerical simulation

1. Introduction – description of the simulated research model

A typical steel beam-to-column joint of scheme, dimensions and geometry depicted in Fig. 1 is the subject of our analysis. The joint represents a connection between the cantilever column made of IPE 360 I-beam and a cantilever beam

---
[1] Corresponding author: Mariusz Maślak, Cracow University of Technology, Faculty of Civil Engineering, Chair on Metal Structures, Warszawska 24, 31-155 Cracow, phone: 126282033, e-mail: mmaslak@pk.edu.pl

[2] Michał Pazdanowski, Cracow University of Technology, Faculty of Civil Engineering, Department for Computational Civil Engineering, Warszawska 24, 31-155 Cracow, phone: 126282929, e-mail: michal@l5.pk.edu.pl

made of IPE 240 I-beam at the height of 1 200 mm above the restraint level. The external load is applied as a concentrated force having the value of $P = 60$ kN applied at the distance of $L = 2.00$ m measured with respect to the undeformed face of the beam end plate. This results in the bending moment equal to $M = 120$ kNm applied at the joint face, tensioning the top and compressing the bottom flange of the beam. As visible in Fig. 1, horizontal ribs stiffening the column web have been applied on both sides of the column at the height of both flanges of the beam. The rib thickness is equal to 10 mm in each considered case. No diagonal ribs have been applied.
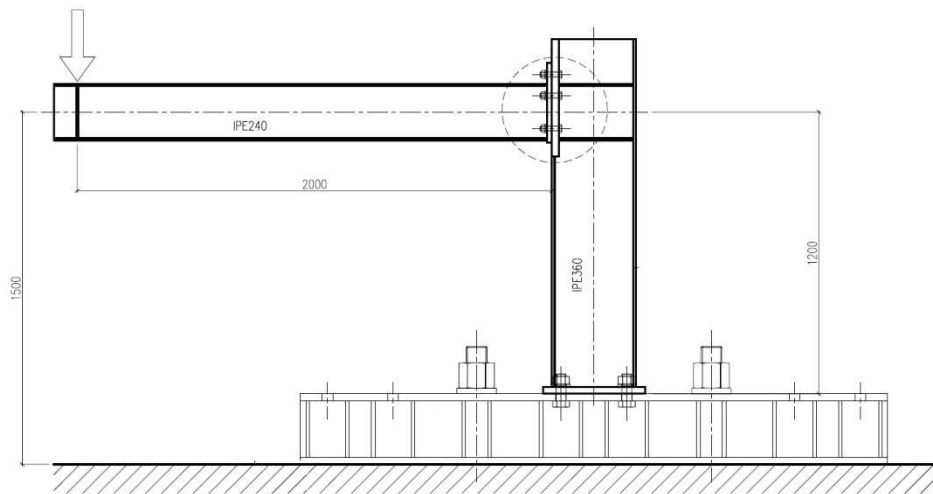

Fig. 1. Scheme, dimensions and load application for the considered joints. The presented stand has been prepared for experimental research conducted at Cracow University of Technology by another research team

In each considered case the end plate is attached to the column flange with $M 20x80$ bolts of 10.9 class spaced in three rows of two bolts each, as depicted in Fig. 2. It was assumed that in the zone directly adjacent to the beam end plate, at the height of 500 mm, measured from the top, the original column flange was replaced by one 30 mm thick, regardless of the joint considered. This allowed for elimination of the influence of this flange on the joint rigidity, observed and quantified in numerical simulations described in this paper. These simulations were performed for four joints of identical geometry, depicted in Fig. 1, but differing in the end-plate thickness. In the joint of the type A this thickness was equal to 20 mm resulting in relatively rigid plate resisting deformation even when subjected to relatively large loads. In the joint of the types B, C and D the end-plate thickness was equal to 10 mm, 8 mm and 6 mm, respectively.
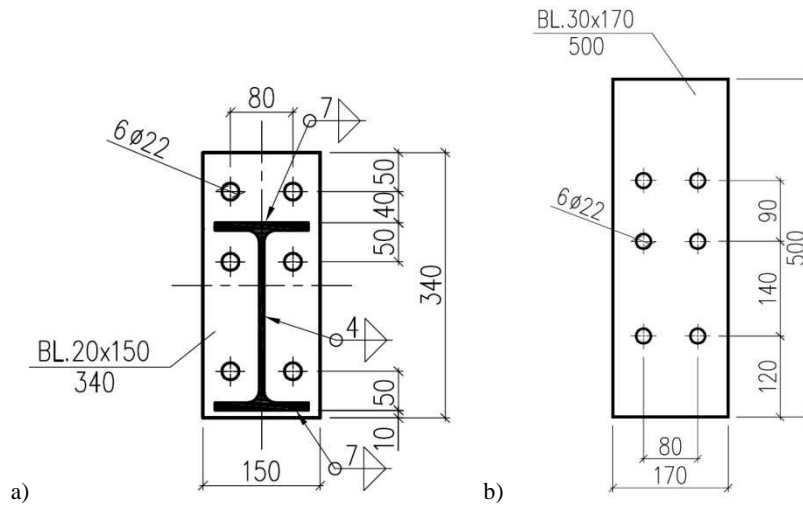
Fig. 2. Bolt location in the joints simulated in present paper and application of fillet welds: a) beam side view towards the end plate, b) column flange view towards the joint (replaced flange part only)
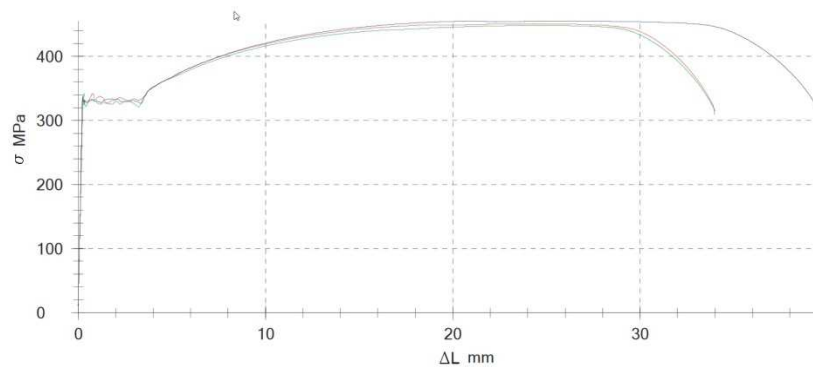

Fig. 3. Independently obtained stress – strain relationship for the structural steel of which all the structural components of joints simulated in present paper have been made

All the components of joints simulated in present paper have been made of structural steel characterized by the $\sigma - \varepsilon$ relationship determined experimentally on three specimens subjected to the uniaxial tension test. The following authoritative average values of material data have been determined:

– for the conventional yield point – $R_{p,0.2} = 328.9$ MPa,

– for the ultimate strength – $R_m = 451.5$ MPa,

– for the longitudinal modulus of elasticity – $E_a = 205.2$ GPa,

– for the limit elongation: in the case of fivefold sample $A_{5,65} = 30.6\%$, and in the case of tenfold sample $A_{11,2} = 23.6\%$.

The selection and calibration of the numerical model parameters listed above have been made by the authors with the intent to verify the assumptions and results of experiments conducted at the Cracow University of Technology by another research team. Detailed elaboration of the results obtained in this experiment is still in preparation. In this research the initial imperfections of the end plate not adhering to the column flange are additionally introduced. The assessment of the influence of these imperfections and various methods of their correction on the real rigidity and bearing capacity of the considered joint is the main goal of that analysis.

2. Characteristics of the numerical model applied

The numerical model developed within the Abaqus [1] computational environment has been applied in order to simulate the behavior of the four joint types of the same geometry, but differing in the end-plate thickness as described above, when subjected to external loads. Eight node brick type C3D8R finite elements with reduced integration and hourglass control have been applied. The total number of degrees of freedom was equal to 403350 – for the model with endplate $20\,mm$ thick, 415392 – for the model with endplate $10\,mm$ thick, 420246 – for the model with end-plate $8\,mm$ thick and 418041 – for the model with end-plate $6\,mm$ thick. The external load has been applied as the vertical traction applied to the cylindrical spacer at the end of beam. The complex contact interactions have been modeled by the contact pairs between the respective interacting surfaces, in a manner analogous to that used in the paper [2]. The „surface-to-surface" contact type has been used throughout the analysis, with friction coefficient $\mu = 0.50$. Each bolt with nut has been modeled as a single unit, while spacers have been modeled independently. The following contact pairs have been created: bolt head – end-plate, bolt shank – end-plate bolt hole, nut – spacer, spacer – column flange, bolt shank – column head bolt hole, end-plate – column flange. The scheme of assumed numerical model is depicted in Fig. 4.
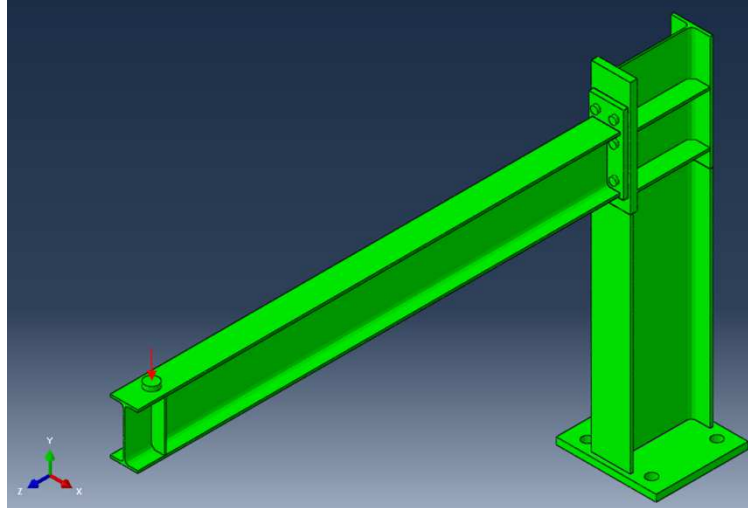
Fig. 4. Numerical model applied to simulate the behavior of joints analyzed in this paper when subjected to external loads

3. The joint destruction forecast depending on the end plate thickness applied

The simulations performed visualized the differences in deformation modes of both constituting components of each node as well as whole surroundings of joint area at limit loads. Observation of differences in the deformation of the end-plate for end-plates substantially differing in rigidity was especially important for the authors. The destruction mode of the A type joint, having the end plate 20 mm thick is depicted in detail in Fig. 5. One may easily observe that this end-plate is so rigid that even when a relatively large bending moment is applied to the joint, deformation of the end-plate is hardly visible even at the ultimate limit state. This suggests the relatively large probability that the joint would fail due to the destruction of the highly stressed bolts located at the external edge of end-plate without any interaction with the relatively undeformed plate, such as, for instance, the lever action amplifying the tensile force in these bolts. The simulation performed by the authors indicated completely different destruction mode of the joint determining its bearing capacity. The limit state was determined by the yielding and deformation of the bottom, compressed, beam flange (Fig. 5), while the bolts remained undamaged. Such behavior should be associated with relatively stringent limitation of effective rotation angle and thus in practical terms deformation corresponding to the nominally rigid work regimen.
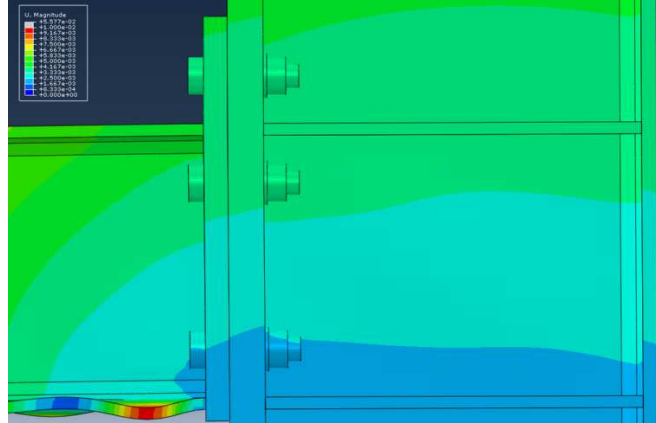
Fig. 5. Ultimate limit state of the A type joint considered here, equipped with $20\ mm$ thick end-plate, attained via yielding of the bottom, compressed, beam flange. The deformation of the beam end-plate in the tensile zone of the joint is hardly visible. The bolts remain undamaged
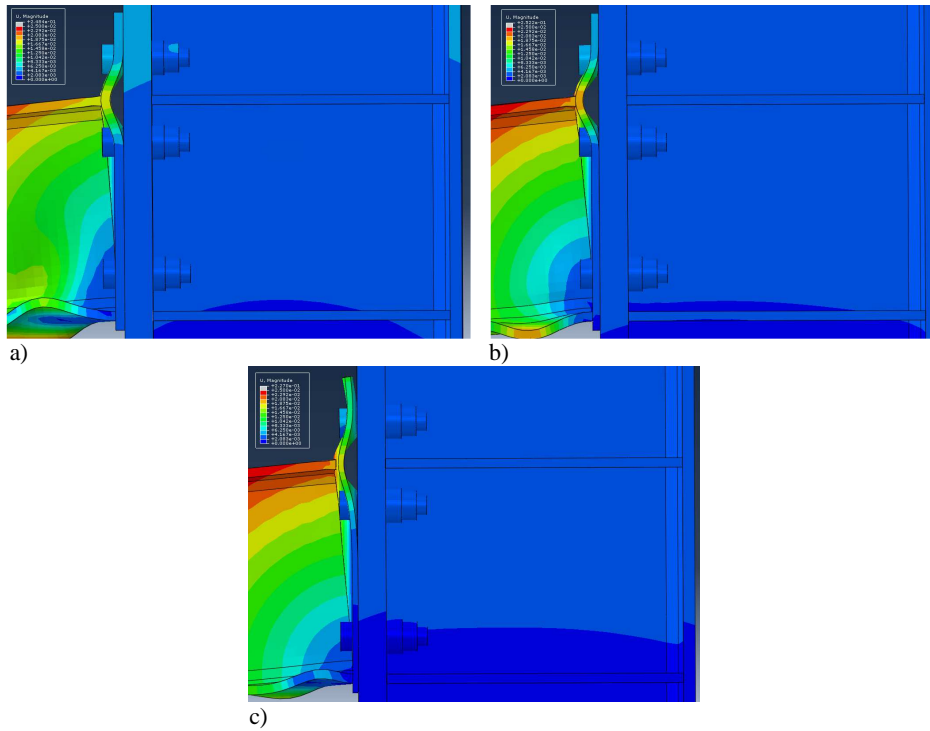

a)

b)

c)

Fig. 6. Joint destruction mode for joints equipped with thin end-plate realized via large deformation of this plate in the tensile zone of the joint, accompanied by the deformation of the compressed bottom flange of the beam: a) B type joint – end-plate 10 mm thick, b) C type joint – end-plate 8 mm thick, c) D type joint – end-plate 6 mm thick

The numerically simulated destruction mode of the joints belonging to the types B, C and D, equipped with relatively thin end-plate, is fundamentally different. The bearing capacity of the whole joint is, to the increasing extent, determined by the deformation of the end-plate in the tensile zone accompanied by the deformation of the bottom, compressed, beam flange (Fig. 6). The maximum displacement of the end-plate face is here always observed at the level of the beam top flange, as this flange, subjected to tension, „pulls" behind the very thin end-plate, susceptible to this type of action in the zone located between the two top rows of bolts, stabilizing its location. It should be noted, however, that this „pulling" action of beam is the strongest in the web plane of the beam and is noticeably weaker outside of its flanges at the distance to the web. This difference, under favorable circumstances, may lead to additional deformations of the end-plate, observed in the plane perpendicular to the frame plane. However, in general due to the substantial resistance to deplanation of the hot rolled beam section, this phenomenon plays secondary, and thus negligible role. Interestingly, with decreasing thickness of the end-plate the deformation associated with top, tensioned, beam flange tends to play increasingly dominant role, while the influence of the compressed bottom flange gradually diminishes.

Detailed analysis of equivalent Huber – von Mises stress distributions on both sides of the end-plate (view towards the column and view towards the beam) yields additional interesting information – Figs. 7–10. The thinner the end-plate the more it deforms. Thus the zones of the highest stresses in the thin plates are usually isolated and localized around the bolt holes. This is the direct result of reaction to the dominating interaction between the plate and bolts prestressing the joint. The more distant surroundings of the bolt holes relatively weakly contribute to the transfer of loads. However, if the end-plate is sufficiently thick the redistribution of equivalent stresses seems to be more pronounced and this in turn makes the cooperation of adjacent regions more efficient. Thence in such situations the highest equivalent stresses do not concentrate around bolt holes but become more pronounced in the adjacent areas as well. This in turn results in grouping of formerly isolated stress concentration zones into much larger areas, and subsequently in relocation of these zones to the area directly affected by the action of top, tensioned, beam flange. This relocation proves that when a thicker plate is applied at the joint the „pulling" of the end-plate by the tensioned beam flange becomes dominant in the general balance of actions, while the action of bolts, dominant in the thin plates substantially loses in importance.
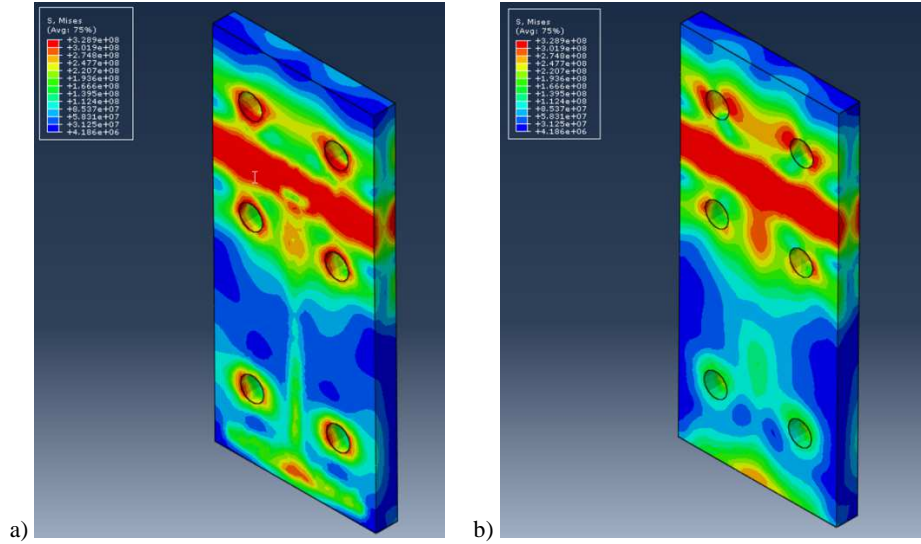
Fig. 7. Distribution of equivalent Huber – von Mises stresses in the end-plate of the A type joint,
20 mm thick: a) view towards the column flange, b) view towards the beam
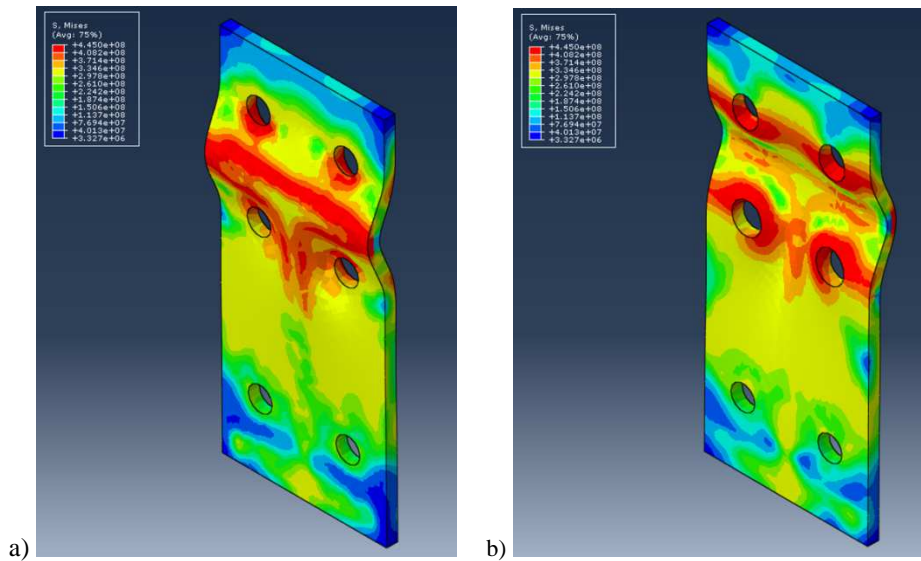

Fig. 8. Distribution of equivalent Huber – von Mises stresses in the end-plate of the B type joint,
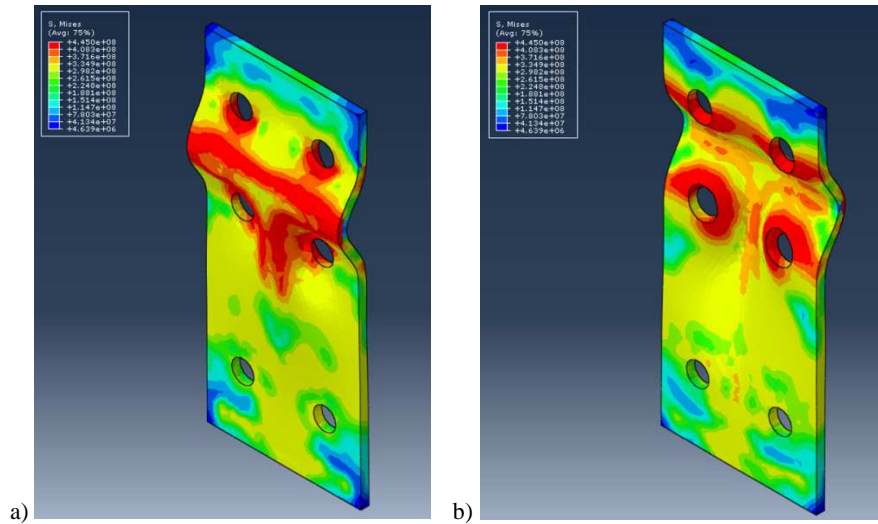10 mm thick: a) view towards the column flange, b) view towards the beam

Fig. 9. Distribution of equivalent Huber – von Mises stresses in the end-plate of the C type joint, 8 mm thick: a) view towards the column flange, b) view towards the beam
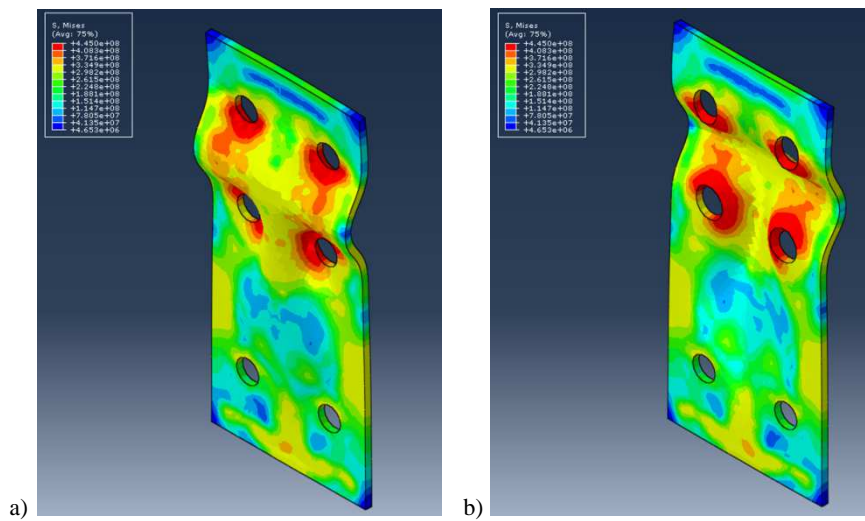

Fig. 10. Distribution of equivalent Huber – von Mises stresses in the end-plate of A type joint, 6 mm thick: a) view towards the column flange, b) view towards the beam

4. Evaluation of modeled joint rigidity

Performed numerical simulations allowed for the determination of the M-φ relationship for each of the joints considered, quantifying the interdependence between the bending moment applied to the joint and the increase in the rotation angle measured between the beam axis and the column axis, related to the

initially straight angle between those two structural component axes. The increase in the rotation angle has been measured in the frame plane, determined before the deformation, thus all the out of plane displacements occurring during the deformation process have been disregarded. No imperfections have been assumed in simulated joint geometry nor in simulated loads. The authoritative M-φ characteristics, a result of current simulation are depicted in Fig. 11. These characteristics, from left to right, pertain to the joints with decreasing rigidity (i.e. A, B, C and D). The borderlines between the zones qualifying the joint as rigid (when the condition $S_{j,ini} \geq 25\left(\dfrac{E_a I_b}{L_b}\right)$ is satisfied), semi rigid and fully flexible (when the condition $S_{j,ini} \leq 0.5\left(\dfrac{E_a I_b}{L_b}\right)$ is satisfied), as recommended in the code PN-EN 1993-1-8 [3] for sway frames, are depicted in Fig. 11 with straight continuous lines. The borderlines have been determined under the assumption that the considered frame represents one half of a typical sway portal frame. This means that the authoritative equivalent beam length was assumed as $L_b = 2 \times 2.0 \text{ m} = 4.0 \text{ m}$.
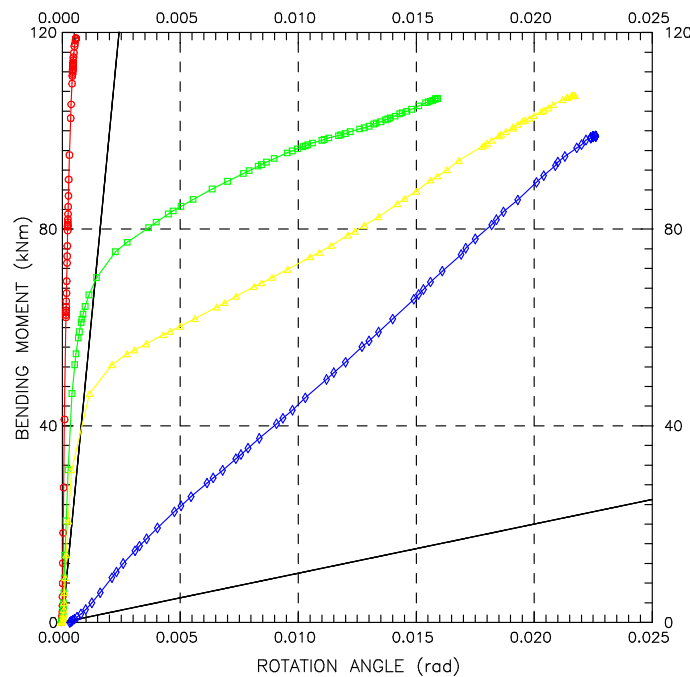

Fig. 11. Resultant M-φ characteristics obtained for the joints analyzed in present paper. The relations presented, from left to right, pertain to the joints of type A, B, C and D. Thus decreasing end-plate rigidity is accompanied by decreasing joint rigidity

It is clearly visible in Fig. 11 that the deformation of A type joint when subjected to load is qualitatively different than the deformation of B and C type joints. In turn the joints of these two types deform in a manner substantially different than the D type joint. Should the joints analyzed in present paper be qualified based on the initial rigidity $S_{j,ini}$, the first three types (i.e. A, B and C) would be assigned to the fully rigid group. In reality, however, the joints belonging to the types B and C attain the full bearing capacity at the relatively large value of rotation angle φ, while the limit value of the same angle in the case of A type joint is much smaller, in general negligibly small. One should also note the qualitatively different behavior of D type joint when subjected to loads. The joint of this type, based on the results of performed simulations is qualified as typical flexible one. Its characteristic is at the same time very close to linear in the whole deformation range, in which it is able to safely resist the loads applied to it. Its initial rigidity, even at the very low values of bending moment applied, is very low, as its value is incomparable with the values determined for other joint types considered here.

Relations depicted in Fig. 11 allow for the determination of bearing capacity of analyzed joints. This proved to be relatively similar for all considered joints. This means that the change in end plate thickness, even so drastic as considered here, exerts unequivocal and clear influence on the resultant joint rigidity. The influence on the bearing capacity, however, is much more subtle.

5. Concluding remarks

It was shown in the paper that the numerical simulation especially on performed on the sufficiently complex computational models may constitute an efficient and effective tool allowing for determination of joint rigidity and bearing capacity, relatively reliable and unequivocal in interpretation. The authors' experience seems to indicate that the M-φ curves – a result of such analysis tend to indicate that the initial rigidity of the considered joints is much higher than the corresponding rigidity determined for the same joints using the classical analytical component method. This conclusion is not surprising. It only confirms the earlier findings reported for instance in [4]. In the bibliography on the subject one may find as well the opinions, that the numerical models may overestimate the joint rigidity, with respect to values arrived at via experiment. This conclusion may hardly be generalized and should be verified by individualized and sufficiently detailed comparisons. However, one should always keep in mind that that every estimate of joint rigidity determined by numerical simulation is highly sensitive to many details preset during the development of numerical model (c.f. for instance [5]). Therefore the validation of results obtained by the authors and presented in this paper, even if only via the application of different computational environment [6] would be highly desirable.

References

[1] Abaqus 6.14: Abaqus/CAE user's guide, Dassault Systèmes, 2014.

[2] Górnik G., Ślęczka L.: Degradation of structural properties in steel joints butt joint loaded in a non monotonic manner, Inżynieria i Budownictwo, 2/2018, pp. 91–94 (in Polish).

[3] PN-EN 1993-1-8: Eurocode 3 – Design o steel structures, Part 1-8: Design of joints.

[4] Jabłońska-Krysiewicz A.: Finite element modeling of the behaviour of steel end-plate connections, Czasopismo Inżynierii Lądowej, Środowiska i Architektury – Journal of Civil Engineering, Environment and Architecture, JCEEA, vol. XXXII, z. 62, 3/II/2015, pp. 173–184, DOI:10.7862/rb.2015.148.

[5] Czaja J., Śliwa R.: Modelling of screw joins with its experimental verification, Archives of Metallurgy and Materials, vol. 52, issue 2, 2007, pp. 267–276.

[6] Maślak M., Pazdanowski M., Woźniczka P.: Numerical validations of selected computer programs in nonlinear analysis of steel frame exposed to fire, AIP Conference Proceedings 1922, 150007-1-150007-9, Published by AIP Publishing, 2018.